RESEARCH ARTICLE

Total control of fat cells from adipogenesis to apoptosis using a xanthene analog

Ching-Hsuan Tung[1]*, Myung Shin Han[1], Jianjun Qi[2]

1 Molecular Imaging Innovations Institute, Department of Radiology, Weill Cornell Medicine, New York, NY, United States of America, 2 Department of Translational Imaging, Houston Methodist Research Institute, Houston, TX, United States of America

* cht2018@med.cornell.edu

Abstract

Overcrowded adipocytes secrete excess adipokines and cytokines under stress, which results in a deregulated metabolism. This negative response to stress increases the possibility of obesity and several of its associated diseases, such as cancer and atherosclerosis. Therefore, a reduction in the number of adipocytes may be a rational strategy to relieve the undesired expansion of adipose tissue. A newly synthesized xanthene analog, MI-401, was found to have two distinct effects on the regulation of the adipocyte's life cycle. MI-401 efficiently down regulated the expression of transcription factors, PPARγ and C/EBPα, and lipogenesis proteins, FAS and FABP4. This down regulation resulted in the inhibition of adipogenesis. Without newly differentiated adipocytes, the total number of adipocytes will not increase. In addition to this inhibitory effect, MI-401 was able to actively kill mature adipocytes. It specifically triggered apoptosis in adipocytes at low micro molar concentration and spared preadipocytes and fibroblasts. These dual functionalities make MI-401 an effective agent in the regulation of the birth and death of adipocytes.

Introduction

Adipocytes are the primary cell type in fat tissue. These cells collect excess triglycerides and place them into lipid droplets as energy depots. The total adipose tissue mass depends on the number and size of the adipocytes. During childhood and adolescence, adipocytes arise through adipogenesis from fibroblast-like progenitor cells, and the initial adipocyte generation process becomes static post adolescence.[1] Under normal metabolic conditions, adipocytes have a mean lifespan of 10 years.[2] Only 10% of all adipocytes undergo a yearly renewal process, which is tightly balanced between the adipogenesis of preadipocytes and the apoptosis of adipocytes. However, recent studies suggested that a prolonged period of obesity may cause the body to recruit new preadipocytes and stimulate their differentiation into mature adipocytes, increasing the number of total adipocytes.[3, 4] As the number increases, the continuous deposit of triglycerides further cause adipocytes to grow in size.[5] The overexpansion of adipose tissue yields to severely dysfunctional adipocytes that secrete adipokines and cytokines, such as leptin and adiponectin, and cause alterations to their normal metabolism.[6] Obesity,

therefore, has been linked to many chronic diseases and metabolic disorders including diabetes[7], atherosclerosis[8, 9] and cancer.[10, 11]

Control over the unhealthy expansion of adipose tissue would pose a significant benefit to the management of obesity and its associated diseases. Current anti-obesity drugs are primarily based on appetite suppression and reduction in fat uptake.[7, 12] The treatments are able to change the size of adipocytes, which result in marked weight loss, but the total number of adipocytes remains the same.[1] Once the treatment stops, the contracted adipocytes expand to regain their original size. Therefore, although weight management is an excellent step towards obtaining a healthy metabolism, it may not be the best solution for all obese adults. A reduction in the total number of adipocytes, by cutting their supply or reducing their inventory, may be a more effective strategy in regulating the expansion of unhealthy fat tissue.

Adipocytes are terminally differentiated cells. When induced by adipogenic stimuli, the committed preadipocytes undergo mitotic clonal expansions and become adipocytes. Inhibitors that block adipogenesis, both natural products[13–18] and synthetic molecules[19–22], have been proposed to prevent the differentiation of these preadipocytes. Furthermore, reagents that can push mature adipocytes into apoptosis have also been suggested as a possible strategy in controlling obesity.[23, 24] Unfortunately, possible drug candidates have been restricted to natural products and plant extracts due to an inadequate understanding of the adipocyte's apoptotic mechanism.[25–32] A few natural molecules and combinations of those molecules have been identified as apoptosis triggers and differentiation inhibitors, but their efficacy is mild. Often, a high concentration, greater than 100 μM, is needed to obtain an appreciable effect in culture.[25–28, 31–34] In 2015, sodium deoxycholate (SD) was approved by the FDA to reduce the unwanted submental fat, a very different compound from those previously available.[35–37] SD acts like a detergent, causing adipolysis (or adipocytolysis) when injected directly into the area with extra fat tissue.[36, 38] SD lyses the adipocyte's membrane, which is deficient in cell associated proteins, resulting in necrosis.[37, 38] The usage of SD has been limited to the removal of local fat tissue because the required active dose is high, 2 mg/ml (~ 5 mM) and 0.2 ml/cm^2.[37]

Planar tricyclic oxygen containing xanthene molecules are known to have various bioactivities.[39–42] For example, a fluorescent xanthene dye, Rose Bengal, is an effective photosensitizer for photodynamic therapy.[43] Previously, we reported a membrane sensitizing Rose Bengal derivative, which killed cancer cells by immediate membrane lysis when insonated by ultrasound,.[44] Several derivatives were later synthesized to study their membrane sensitizing property in cancer cells. Since adipocyte contains a unique cell membrane, one synthesized molecule, MI-401 (2, 3, 4, 5- tetrachloro- 6- (6- hydroxy- 2, 4, 5, 7- tetraiodo- 3- oxo- 3H-xanthen- 9- yl)—N- (2- hydroxyethyl) -benzamide; Fig 1), was tested with adipocytes. Unexpectedly, it was found that MI-401 regulates the adipocyte's life cycle in two ways. MI-401 effectively inhibits the adipogenesis process by differentiation arrest, $IC_{50} = 3$ μM, and kills mature adipocytes through the induction of apoptosis, $EC_{50} = 5$ μM.

Materials and methods

Reagents and cells

Sodium deoxycholate (SD), 4,5,6,7-tetrachloro-2',4',5',7'-tetraiodofluorescein, N,N,N',N'-Tetramethyl-O-(1H-benzotriazol-1-yl)uronium hexafluorophosphate, O-(Benzotriazol-1-yl)-N,N,N',N'-tetramethyluronium hexafluorophosphate (HBTU), diisopropoyl ethyl amine (DIEPA), and Dimethyl sulfoxide (DMSO) were obtained from Sigma-Aldrich (St. Louis, MO, USA). All other solvents, including dimethyl formamide (DMF), dichloromethane (DCM), and methanol (MeOH), were purchased from Thermo Fisher (Waltham, MA).

The triglyceride quantification kit AdipoRed[TM] was obtained from Lonza Walkersville (Walkersville, MD). CellMask[TM] Plasma Membrane Stain with DAPI, and LipidTox[TM] DeepRed neutral lipid stain were purchased from Thermo Fisher. The LumiGLO® reagent used in Western blot studies, and antibodies against the fatty acid-binding protein4 (FABP4), peroxisome proliferator-activated receptor γ (PPARγ), CCAAT element binding protein α (C/EBPα), fatty acid synthase (FAS) and β-Actin were obtained from Cell Signaling Technology (Beverly, MA, USA). The BCA protein assay kit and M-PER were purchased from PIERCE (Rockford, IL, USA). CellTiter 96® AQ$_{ueous}$ One solution (MTS) Cell Proliferation Assay kit, ApoOne® Homogeneous Caspase 3/7 assay kit and CytoTox-One[TM] Homogeneous Membrane Integrity Assay kit were from Promega (Madison, WI, USA).

3T3-L1 preadipocytes (passage 7 to 8) and culture media were obtained from Zen-Bio (Research Triangle Park, NC, USA). Only passage 8 to passage 11 were used in the study. NIH3T3 fibroblast cells were obtained from ATCC (Manassas, VA, USA) and maintained in a DMEM medium with 10% FBS at 37˚C and 5% CO_2.

Synthesis of MI-401 (2,3,4,5-tetrachloro-6-(6-hydroxy-2,4,5,7-tetraiodo-3-oxo-3H-xanthen-9-yl)-N-(2-hydroxyethyl)-benzamide)

MI-401 was prepared following a described procedure.[44] Briefly, 4,5,6,7-tetrachloro-2',4',5', 7'-tetraiodofluorescein (0.5 mmol) was activated by HBTU (0.5 mmol) in DIEPA/DMF (2/3, 5 ml) and stirred at room temperature (RT) for 4 hours. 2-Aminoethanol (1.5 mmol) was then added and reacted overnight at RT. The solvent was removed under vacuum. The residue was extracted with DCM and washed with brine, dried over anhydrous sodium sulfate and concentrated. It was then purified by a silica gel column, and eluted with DCM, DCM/MeOH = 10/0.5 and 10/1 (V/V), to give a pale yellow solid product (yield 31%).
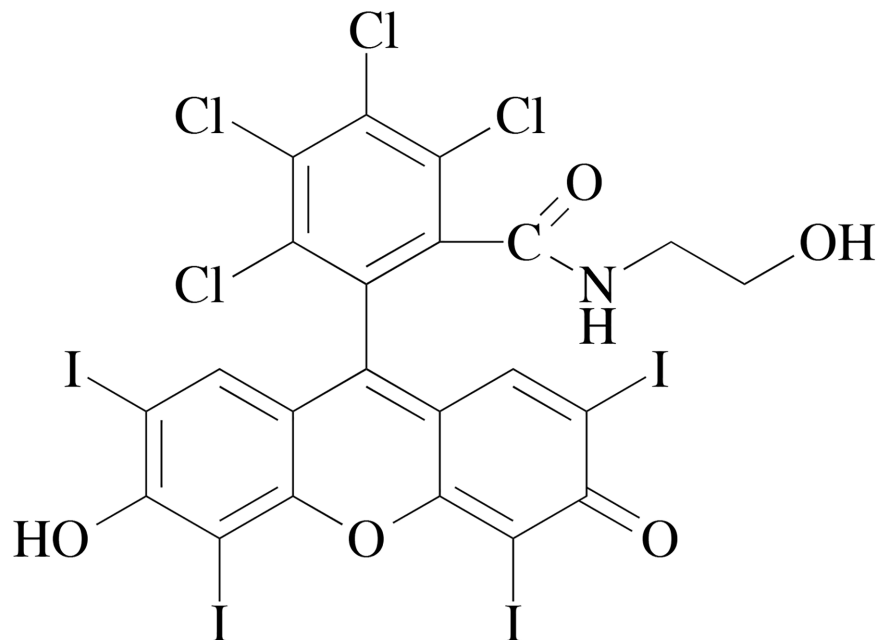
MI-401

Fig 1. The chemical structure of MI-401.

General culture and differentiation conditions for 3T3-L1 cells

3T3-L1 preadipocytes were grown in 3T3-L1 Preadipocyte Medium (PM-1-L1) with 5% CO_2 at 37˚C for two to three days to reach confluence. The medium was replaced with a 3T3-L1 Differentiation Medium (DM-2-L1) to stimulate differentiation. After 3 days in DM-2-L1, the differentiated cells were matured with 3T3-L1 Adipocyte Maintenance Medium (AM-1-L1) for an additional 3 days. This general protocol was used in all experiments, but adjusted with various treatments. The detailed experimental scheme is described in each figure.

MI-401 Stock solution preparation

MI-401 was dissolved in pure DMSO (Sigma) to obtain 1 to 20 mM stock solutions. Prior to each cell experiment, the MI-401 stock solution was diluted to the desired concentration using cell culture medium. After dilution, the final DMSO concentration was no higher than 1%. The DMSO solution (1%) presented no significant toxicity to the tested cells.

MTS assay for cell viability and EC_{50}

Cells (3,000/well) were seeded in a 96-multiwell plate (Corning Costar) with complete medium (100μL per well), and incubated at 37˚C, with 5% CO_2. The cells were then treated with various concentrations of MI-401 or SD (1–400 μM) for the indicated time periods. The MTS assays in a 96-well plate were done with a CellTiter 96Ⓡ AQ_{ueous} reagent (20 μl, Promega) in a culture medium (100 μl). The plates were incubated at 37˚C for 4 h. Absorbance was measured at 490 nm using a microplate reader (Infinite M1000 Pro, Tecan, Männedorf, Switzerland). The experiments were done in at least triplicate.

Measurement of lipid accumulation

The triglyceride accumulation was quantitated after the cells underwent treatments with different amounts of MI-401 for 1 or 2 days. The cells were rinsed with PBS prior to the commencement of the assay. An AdipoRed[TM] solution (30 μL) was added to each well, homogenized by pipetting, and then incubated for 10–15 min at RT. The amount of triglyceride was measured using a fluorescent plate reader (Infinite M1000 Pro, Tecan) with a 485 nm excitation and a 572 nm emission. The experiments were done in triplicate.

Lipid stain for fluorescence microscopy

The cells were washed twice with the phosphate-buffered saline (PBS), fixed with 3.7% formaldehyde solution for 10 minutes at RT, and then rinsed gently 2–3 times with a PBS buffer to remove residual formaldehyde. LipidTox[TM] Deep Red stain solution (1:200 in a buffer) was added to the wells and incubated at RT for 30 minutes before fluorescence imaging using a Cy5 filter (ex = 650 nm, em = 670 nm).

Plasma membrane and DAPI staining for Cell death image

The plasma membrane and nucleus were stained using a CellMask[TM] Plasma Membrane Stain with DAPI (Thermo Fisher) in accordance with the manufacture's protocols for 5–10 min at 37˚C. The cells were imaged with a fluorescent microscope (Evos FL, Thermo Fisher) using GFP and DAPI filters.

Cell death mechanism study

Caspase3/7 activity assay was done with the ApoOne Homogeneous Caspase 3/7 assay (Promega) following the manufacturer's instructions. Matured adipocytes were treated with SD (50 μM) or MI-401 (10 μM) in 100μL of AM-1-L1 (3T3-L1 Adipocyte Maintenance Medium) and then Apo-One Caspase-3/7 Reagent (100 μL) was added to each well. These wells were gently mixed using a plate shaker at 300 rpm for 30 sec. The fluorescence reporting the caspase activity was monitored using a fluorescence plate reader (Infinite M1000 Pro, Tecan) for 18 hours at RT with a 499 nm excitation and 521 nm emission. The experiments were done in triplicate.

LDH release was assayed using the CytoTox-ONE kit (Promega) following the manufacturer's instructions. The cells, in a 96-well plate, were added with a CytoTox-ONE Reagent (100 μL). The plate was gently shaken at 300 rpm for 30 sec, incubated at 22°C for 10 min, and then stopped by a stopping solution (50μL). The fluorescence was measured using a fluorescence plate reader (Infinite M1000 Pro, Tecan) with a 560 nm excitation and a 590 nm emission. Percent cytotoxicity was calculated following the manuscript's instructions. Percent cytotoxicity = 100 x (Experimental–Culture medium background)/(Maximum LDH release–Culture medium background). The experiments were done in triplicate.

Preparation of cell lysates and Western blotting

After treatments, the cells were washed twice with PBS and lysed with M-PER (PIERCE) on ice for 5 min. The lysates were centrifuged at 14,000x g for 5 min, and the supernatants were collected. Protein concentrations were determined using a BCA protein assay kit (PIERCE). The proteins were separated by SDS-PAGE (4~12%) and transferred to nitrocellulose membranes. The membranes were washed with 0.05% (vol/vol) Tween 20 in PBS, followed by blocking with 5% (wt/vol) non-fat dried milk. The membranes were incubated overnight with antibodies specific for C/EBPα (1:1000), PPARγ (1:1000), FAS (1:1000), and FABP4 (1:1000) and β-actin (1:5000) at 4°C. The membranes were then washed with PBS and exposed to secondary antibodies coupled with horseradish peroxidase (Anti-rabbit IgG, HRP-linked antibody, Cell Signaling) for 2 hours at RT. The membranes were washed three times for 5 min with PBS at RT. Immunoreactivities were detected by an enhanced LumiGLO® reagent (Cell Signaling) and documented using the F-Pro imaging system (Bruker, Billerica, MA).

RNA isolation and qPCR analysis

In a separate set of cells, 3T3-L1 cells were treated using the same method for the Western blot analysis. At the designated time points, the total RNA from the control or MI-401 treated 3T3-L1 cells was extracted using a Direct-zol RNA MicroPrep kit with Trizol® reagent (Zymo) following the manufacturer's instruction. Each RNA sample (1μg) was reverse transcribed to cDNA using iScript Reverse Transcription Supermix (Bio-Rad, Hercules, CA).[45] For RT-qPCR, 2 μl of a 1:10 dilution of the cDNA was used per well in a 10 μl reaction, along with 1 μl of primer set (300 nM) and 5 μl of iTaq^{TM} Universal SYBR Green Supermix (Bio-Rad). The reactions were run in triplicate at least on a StepOnePlus Real-Time PCR Detection System (Applied Biosystems, Foster City, CA) with the following protocol: 95°C (2 min), 40 cycles of 95°C (15 s) and 60°C (60 s). All primers were purchased from Integrated DNA Technologies (Coralville, IA). 18s rRNA and β-Actin were used as reference housekeeping genes for normalization and quantification using the 2-ΔΔC(t) method [46]. The primer sequences used were [20, 30]: FABP4: sense 5′-AGTGGGAGTGGGCTTTGCCA-3′ and antisense 5′-GGGCCCCGCCATCTAGGGTTA-3′; C/EBPα: sense, 5′-TTACAACAGGCCAGGTTTCC-3′ and antisense 5′-CTCTGGGATGGATCGATTGT-3′; FAS: sense 5′-TTGCTGGCACTACAGAATG

`C-3'` and antisense `5'-AACAGCCTCAGAGCGACAAT-3'`; PPARγ: sense `5'-GGTGAAACTC`
`TGGGAGATTC-3'` and antisense `5'-CAACCATTGGGTCAGCTCTC-3'`; β-Actin: sense `5'-G`
`GTGAAGGTCGGTGTGAACG-3'` and antisense `5'-GGTAGGAACACGGAAGGCCA-3'`; 18s
rRNA; sense `5'-CTTAGAGGGACAAGTGGCG-3'` and antisense `5'-ACGCTGAGCCAGTCAG`
`TGTA-3'`.

Statistical analysis

All values are presented as means ± standard deviation. P-values <0.05 were considered statistically significant. Statistical significance was determined using a student's t-test. All analyses were performed using the GraphPad Prism program (version 7, La Jolla, CA, USA).

Results and discussion

MI-401 killed mature adipocytes at low µM concentration

SD is currently the only FDA approved drug for the treatment of excess local fat tissue; thus, the cell-killing efficacy of MI-401 was compared to SD using mature 3T3-L1 adipocytes as a model. 3T3-L1 preadipocytes were grown in an adipocyte differentiation medium for 3 days. These cells were then maturated in an adipocyte maintenance medium for an additional 3 days. Once matured, MI-401 and SD were added to the adipocyte's maintenance medium. The cells were then analyzed one or two days after treatments (Fig 2A). Microscopic examination at day 2 found significant morphological changes in the MI-401 (10 µM) treated cells, which were small, dense, and rough (Fig 2B). In contrast, no difference was observed between the untreated mature adipocytes and the SD (10 µM) treated cells. The morphology was clearly different once the administered concentration of SD was raised to 50 µM. The viability of the adipocytes with MI-401 (10 µM) was down to 30% on day 1 and 10% on day 2 (Fig 2C); while SD (50 µM) treated groups still had 70% or 53% of viable cells one or two days after treatment.
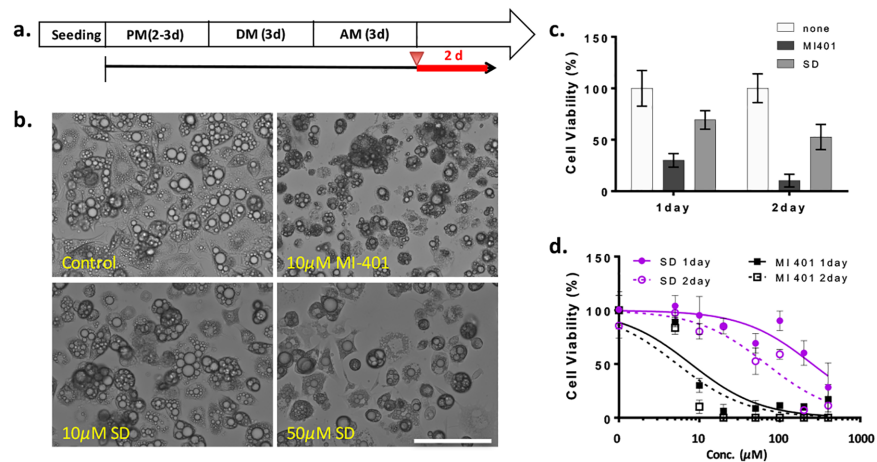

Fig 2. Effect of SD and MI-401 on mature adipocytes. (A) 3T3-L1 cells were cultured in preadipocyte medium (PM), differentiated in differentiation medium (DM), and then maturated in adipocyte maintenance medium (AM). Drugs were added at day 3 after maturation (indicated by red arrowhead). The treatments lasted for 1 or 2 days (Red line). (B) Representative images of mature 3T3-L1 cells treated with MI-401 (10 µM) or SD (10 or 50 µM). Scale bar = 100 µm. (C) Comparison of cell viability of MI-401 (10 µM) and SD (50 µM) treated adipocytes. Data is presented as mean ± standard deviation (n $\geq$ 3). (D) Viability of cultured adipocytes treated with SD or MI-401. The determined EC_{50} for MI-401 after 1-day or 2-day of treatment was 7.9 or 5.3 µM, respectively; and for SD after 1-day or 2-day of treatment was 253.8 or 52.8 µM, respectively. Data is presented as mean ± standard deviation (n $\geq$ 3).

https://doi.org/10.1371/journal.pone.0179158.g002

Subsequent systematic viability studies showed the EC_{50} of MI-401 and SD at post treatment day 2 to be 5.3 and 53 μM, respectively (Fig 2D). The EC_{50} of MI-401 on day 1 was 7.9 μM.

MI-401 triggered apoptosis in mature adipocytes

When compared to the clinically approved SD, MI-401 proved to be approximately 10 times more effective in killing mature adipocytes. In addition to its stronger killing efficacy, a difference in the cell morphology between the treated groups was observed. This difference suggests that the treated cells may have died through different death pathways (Fig 2B). To better visualize the cell's morphology, cells were co-stained with CellMast™ Plasma membrane stains and DAPI nuclear stains 2 days after treatment (Fig 3A and 3B). When compared to untreated mature adipocytes, SD treated cells are about the same in size, but possess a substantially lower
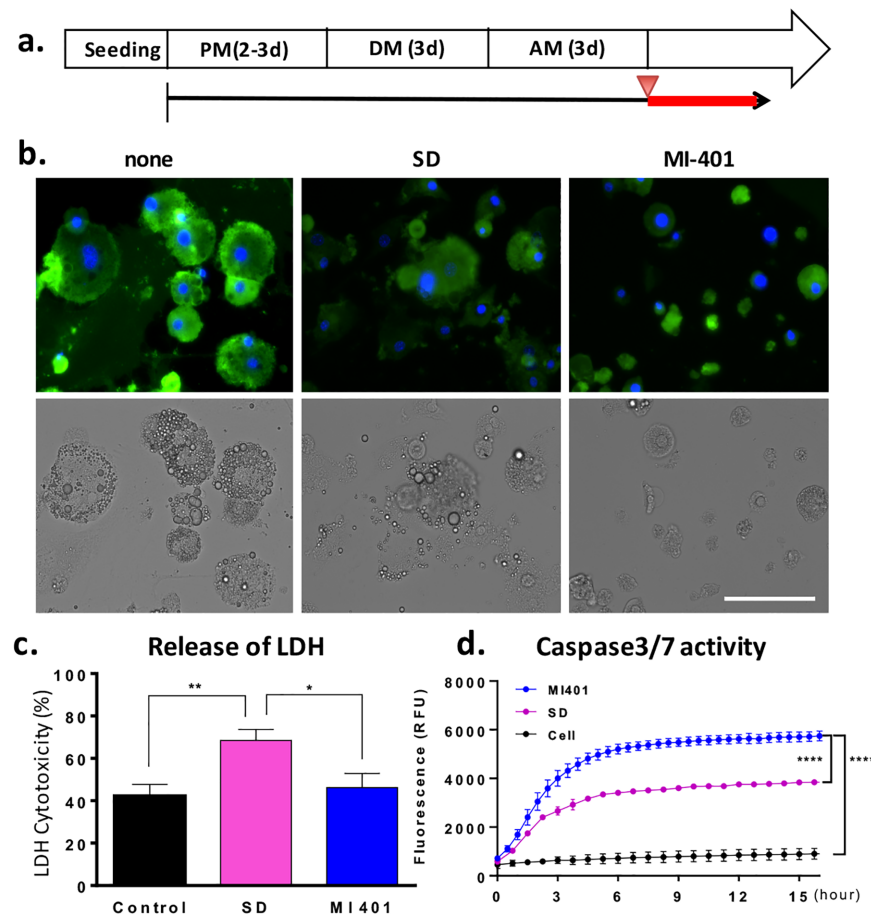

Fig 3. Death mechanism of SD and MI-401 treated adipocytes. (A) 3T3-L1 cells were cultured in preadipocyte medium (PM), differentiated in differentiation medium (DM), and then maturated in adipocyte maintenance medium (AM). SD and MI-401 was added at day 3 after maturation (red arrowhead). The drug treatments lasted 2 days (Red line). (B) Representative images of mature 3T3-L1 cells treated with MI-401 (10 μM) or SD (50 μM). The cell membrane was stained with CellMask™ Plasma Membrane Stain (Green) and the nucleus was stained with DAPI (Blue). Scale bar = 100 μm. (C) Quantitative analysis of necrosis associated LDH release 4 hrs after SD (50 μM) or MI-401 (10 μM) treatment. The LDH released from the total lysed cells was set as 100% LDH cytotoxicity. The untreated adipocytes were used as the negative control. Data is presented as mean ± standard deviation (n = 3). (Unpaired t-test, ** P < 0.005, * P < 0.05) (D) Time course of caspase 3 and 7 activity after SD treatments (50 μM) or MI-401 (10 μM). The fluorescence signal representing caspase 3/7 activity was determined over 18 hours using a fluorescence plate reader. Data is presented as mean ± standard deviation (n = 3). (Paired t-test, **** P ≤ 0.001).

membrane fluorescence intensity. This lowered fluorescence suggests a partial solubilization of the membrane (Fig 3B). Additionally, upon further observation, the lipid droplets appear to have diminished from the cytoplasm. In contrast, MI-401 treated cells have become smaller. Apoptotic characteristics such as cytoplasm shrinkage, nucleus condensation, cell debris and the disappearance of lipid droplets were observed.

SD is known to destroy adipocytes by breaking down or solubilizing cell membranes[37, 47]; therefore, a lactate dehydrogenase (LDH) release assay was selected to study the integrity of the plasma membranes post treatment. As expected, SD treated cells exhibited a significant release of cytosolic LDH which was ~70% over the background value. MI-401 treated cells, however, were only about 25% higher (Fig 3C). The results of this assay suggested that MI-401 does not affect adipocytes by lysing the plasma membrane as SD does. An apoptosis fluorescence assay was then conducted to determine the activity of triggered apoptotic enzymes, caspase 3 and caspase 7. The caspases' activity of the MI-401 treated group steadily increased over the measuring period, and the determined signal was significantly higher than that of the SD treated group (Fig 3D). These experimental results further indicate that MI-401 is an effective apoptosis initiator.

MI-401 inhibited the differentiation of preadipocytes

MI-401 was then checked for its inhibition potential of adipogenesis. 3T3-L1 preadipocytes were seeded and grown to confluence in a preadipocyte maintenance medium for 2–3 days. Thereafter, the cells were cultured in a differentiation medium containing different amounts of MI-401 for one or two days (Fig 4A). Following a 3-day differentiation period, the cells were further cultured in an adipocyte maintenance medium for an additional 3 days and analyzed for their lipid contents. As seen in Fig 4B, the fully differentiated 3T3-L1 adipocytes were rich in large lipid droplets. A two-day incubation with 10 μM of MI-401 in a differentiation medium, almost completely stopped the occurrence of lipogenesis (Fig 4B) in the treated cells. A triglyceride (TG) quantification assay was preformed to determine its IC$_{50}$ after 1-day and 2-day treatments, which resulted in 3.2 and 2.5 μM, respectively (Fig 4C). Importantly, under testing conditions, this differentiation-arresting drug was found to be non-toxic to differentiating preadipocytes (Fig 4C).

MI-401 blocked the early steps of adipogenesis

Following the observation of a strong suppression of lipid deposition during the differentiation, the regulation of four key factors, including two transcription factors: peroxisome proliferator-activated receptor-gamma (PPARγ) and CCAAT/enhancer-binding protein alpha (C/EBPα), and two lipogenesis players: fatty acid synthase (FAS) and fatty acid binding protein 4 (FABP4),[48] that participated in the adipogenic progression were analyzed by Western blotting and qPCR to understand the possible mechanism of adipogenesis arrest. MI-401 (10 μM) was added to the preadipocyte phase or to the differentiation phase. The cells were collected at different stages and subjected to analysis (Fig 5A). The Western results showed that all four factors had low values at the normal preadipocytes stage; however, when the cells began differentiating, the transcription factors, PPARγ and C/EBPα, were highly upregulated (Fig 5B). FAS and FABP4 were also observed to be upregulated but to a lesser extent. After the cells' completion of their differentiations, FAS and FABP4, which participated in lipid synthesis, were further expressed for lipid synthesis and deposition. No difference of expression was observed when preadipocytes were treated with MI-401. Nonetheless, when MI-401 was included in the differentiation medium, the expressions of PPARγ, C/EBPα, and FAS by the differentiating preadipocytes were completely blocked. The expression of FABP4 was also
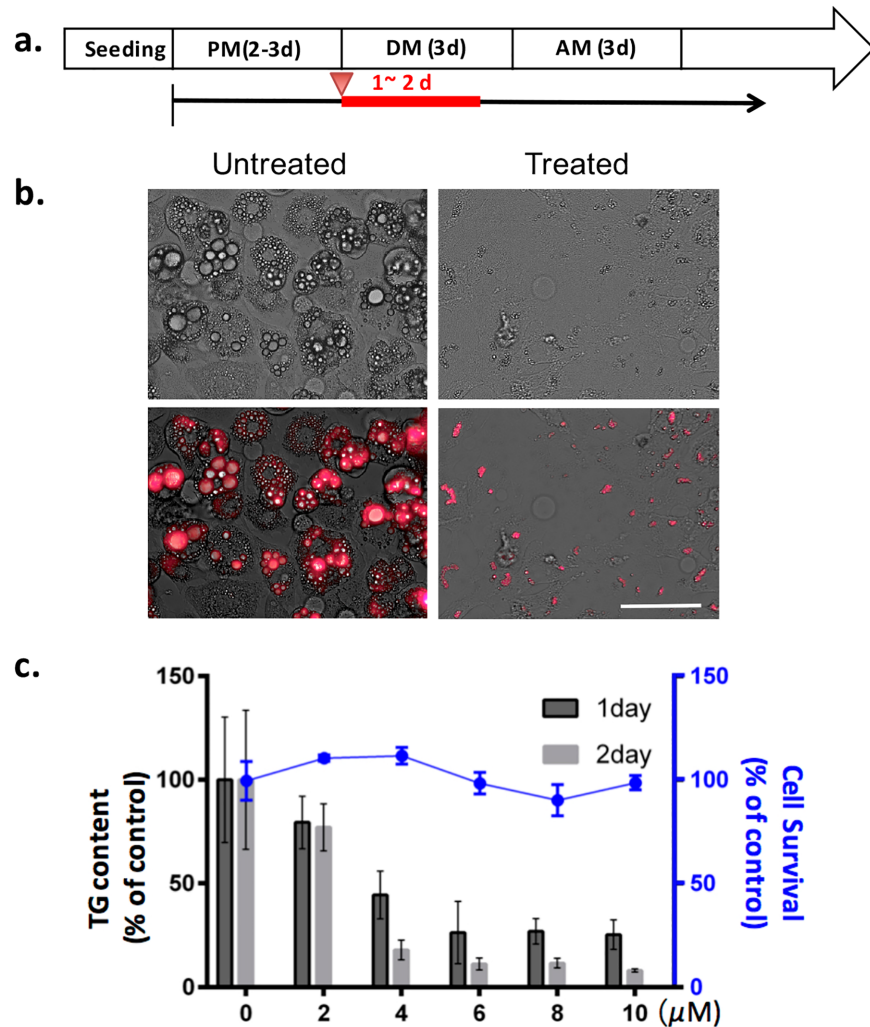
Fig 4. Inhibitory effect of MI-401 during the early stage of adipogenic differentiation. (A) 3T3-L1 cells were cultured in preadipocyte medium (PM) for 2–3 days, and then treated with MI-401 in the differentiation medium (DM) for the indicated time periods (Red line). The cells were continuously cultured in an adipocyte maintenance medium (AM) for an additional 3 days post differentiation. (B) Representative images of the lipid stain in the untreated and treated 3T3-L1 adipocytes. The cells were stained with HCS Lipdox[TM] lipid stain prior to imaging. Scale bar = 100 μm. (C) Quantitative analysis of triglyceride accumulation with MI-401 treatment (black bars and left Y-axis) and cell viability after treatments (blue line and right Y-axis). Data is presented as mean ± standard deviation (n $\geq$ 3). Based on triglyceride content, the IC_{50} of MI-401 with 1-day or 2-day treatment was 3.2 and 2.5 μM, respectively.

significantly down regulated. The suppression of these factors was maintained even after the media was switched to an adipocyte maintenance medium. These results suggest that once the differentiation process is arrested, it cannot be quickly recovered.

To further confirm the regulation of these four factors, RT-PCR was used to quantitate the relative mRNA in all tested conditions (Fig 5C). It was found that the mRNA results corroborated with the Western protein analysis. High mRNA levels of PPARγ and C/EBPα transcription factors were observed in normal differentiation condition and maturation condition, while high mRNA levels of FAS and FABP4 lipogenesis factors were increased in the normal maturation stage. As expected, MI-401 treatment effectively suppressed all four factors at the transcriptional level.
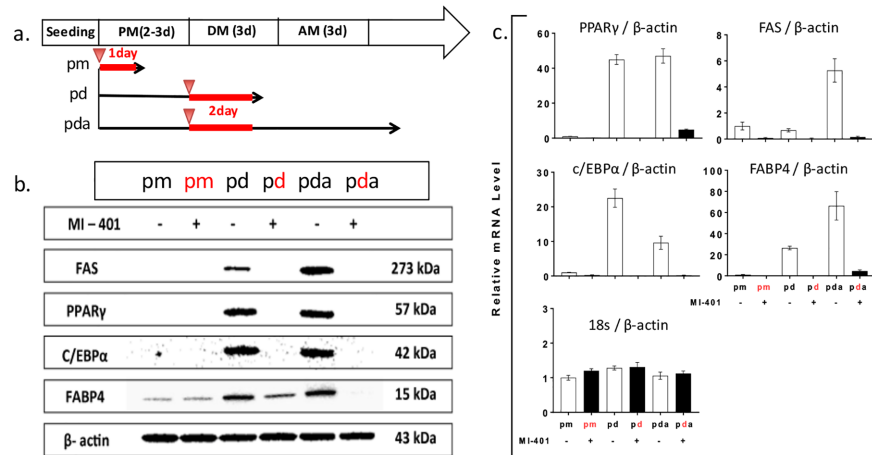
Fig 5. Effect of MI-401 on adipogenic gene expression in different stages of growth. (A) MI-401 (10 μM) was added to the preadipocyte maintenance medium (pm group), or differentiation medium (pd group). The cells were harvested right after the treatment. In the third set of cells (pda group), MI-401 was added to the differentiation medium for 2 days, and then the cells were cultured in the adipocyte maintenance medium for additional 3 days. The red letter indicates the drug treated groups, and the red line indicates the duration of the treatment. (B) Representative Western blot analysis showing the effect of MI-401 on PPARγ, C/EBPα, FAS and FABP4. (C). Relative mRNA level of PPARγ, C/EBPα, FAS and FABP4. Results were expressed relative to untreated cells after normalized to β-actin. Data are expressed as the mean ± standard deviation. Black bar = with MI-401, empty bar = without MI-401.

MI-401 is less cytotoxic to preadipocytes and fibroblast

MI-401 has proven its efficiency in inhibiting adipogenesis. Subsequent studies were done to understand the extent of its cytotoxicity in preadipocytes and normal fibroblasts. To determine it's EC_{50}, 3T3-L1 preadipocytes were seeded and cultured for two days in a preadipocyte maintenance medium together with various amounts of MI-401 (Fig 6A). Fibroblasts (NIH3T3) were also treated with MI-401 in its optimal culture condition. Both cell types remained unharmed and healthy when exposed to a low concentration of MI-401 (10μM). However, the 3T3-L1 preadipocytes were negatively affected in a 50 μM concentration, while NIH3T3 cells retained their health (Fig 6B). The EC_{50} for 3T3-L1 preadipocyte and NIH3T3 cells on day 2 was determined to be 49 and 169 μM, respectively (Fig 6C and 6D).

MI-401 is a bifunctional drug to control adipocytes

The above results suggest that MI-401 may be useful as a bi-functional drug for the management of adipocytes (Fig 7). MI-401 has proven to efficiently kill mature adipocytes by initiating the death pathway. Unlike SD, which kills mature adipocytes through cellular membrane lysis induced necrosis, MI-401 acts as an apoptosis inducer and is about 10 times more effective in killing mature adipocytes. When in contact with lean preadipocytes, MI-401 inhibits the adipogenesis process completely. It inhibits the expression of transcription factors C/EBPα and PPARγ, which are key players in mid-phase adipocyte differentiations.[48] Subsequent analyses have indicated that this inhibition tends to occur at a very early phase of differentiation. During normal adipogenesis, the coordination of PPARγ with the C/EBP transcription factor further drive the expression of other adipocyte-specific genes. This includes FABP4, FAS, and several other proteins that participate in the lipogenesis process, which is the final phase of their differentiation into mature adipocytes.[48] The early suppression of C/EBPα and PPARγ by MI-401 has regulated the downstream expression of FABP4 and FAS, which has resulted in
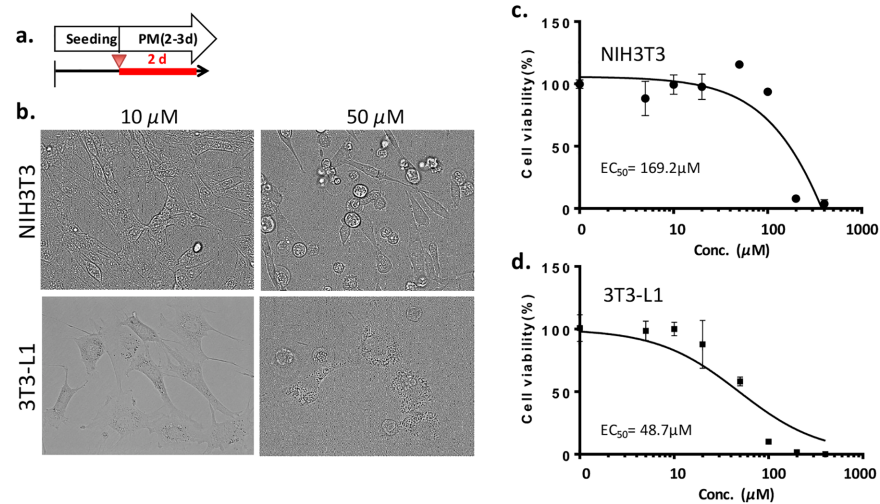
Fig 6. Cytotoxicity of MI-401 on 3T3-L1 preadipocytes and NIH3T3 fibroblast. (A) After seeding, 3T3-L1 preadipocytes were treated with MI-401 (red arrowhead) in a preadipocyte maintenance media (PM) for 2 days (red line). NIH3T3 cells were also treated with MI-401 but in DMEM medium with 10% FBS. (B) Representative images MI-401 (10 or 50 μM) treated 3T3-L1 or NIH-3T3. The NIH-3T3 fibroblasts were healthy at both conditions, but round 3T3-L1 preadipocytes were seen after treated with 50 μM of MI-401. (C) Quantitative analysis of cell viability of NIH-3T3 fibroblast with MI-401. The EC_{50} at day 2 was 169.2 μM. Data are presented as mean ± standard deviation (n = 3). (D) Quantitative analysis of cell viability of 3T3-L1 preadipocytes with MI-401. The EC_{50} at day 2 was 48.7 μM. Data is presented as mean ± standard deviation (n = 3).

https://doi.org/10.1371/journal.pone.0179158.g006

the complete arrest of adipogenesis. MI-401 inhibits the differentiation of preadipocytes, but had no effect on its proliferation. When compared to the compounds reported in literature that inhibit adipogenesis or/and induce apoptosis,[12, 16, 23] MI-401 is the only compound capable of acting at low μM concentrations and be non-toxic to both preadipocytes and normal fibroblasts. \

The EC_{50} of MI-401 for mature adipocytes, preadipocytes, and normal fibroblasts is 5, 49 and 169 μM, respectively. This differential cytotoxicity is extremely beneficial in designing a selective treatment that will not harm normal cells. Based on the unique structure of MI-401, the fundamental differences of the tested cells, and the observed results, it is postulated that MI-401 might have a direct interaction with the fragile lipid droplet membranes. Adipocytes treated with MI-401 lost their lipid droplets quickly, resulting in a sudden burst of triglycerides and other contents within cytoplasm that triggered the cell death process. Conversely, the lean preadipocytes and fibroblasts which have few lipid droplets were more resistant to the treatment. However, this speculation remains to be validated.
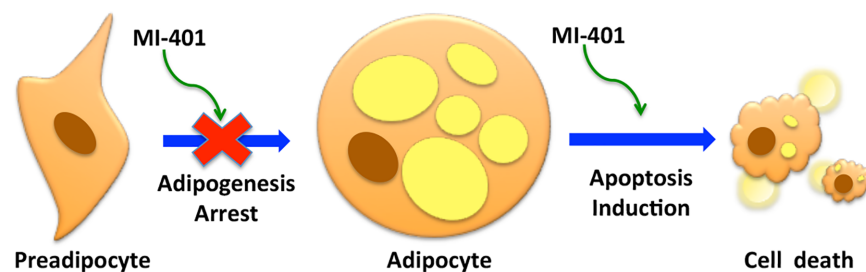

Fig 7. The schematic diagram of the dual functionality of MI-401 to differentiating and matured fat cells. MI-401 inhibits the adipogenesis of preadipocytes, and stimulates apoptosis in adipocytes.

https://doi.org/10.1371/journal.pone.0179158.g007

Conclusion

In summary, MI-401, a newly synthesized molecule with no known biological activity, is a possible drug candidate for the management of excess adipose tissue. MI-401 is an effectual adipogenesis inhibitor with an IC_{50} of 3 μM, and a potent adipocyte killer with an EC_{50} of 5 μM. Like the clinically approved adipolytic SD for mesotherapy, MI-401 could also be potentially applied to the mesoderm to treat local fat tissues. Due to its low EC_{50} to adipocytes, a significantly lower dose is needed to achieve a similar effect. MI-401 is structurally different from other reported analogs and therefore, may provide a new direction for drug development. Further modification and optimization of MI-401 may lead to a new way of controlling fat tissue and treating obesity.

Author Contributions

Conceptualization: MH CT.

Data curation: MH JQ CT.

Formal analysis: MH JQ CT.

Funding acquisition: CT.

Investigation: MH JQ CT.

Methodology: MH JQ CT.

Project administration: CT.

Resources: MH JQ.

Supervision: CT.

Validation: MH JQ CT.

Visualization: MH JQ CT.

Writing – original draft: MH JQ CT.

Writing – review & editing: MH JQ CT.

References

1. Spalding KL, Arner E, Westermark PO, Bernard S, Buchholz BA, Bergmann O, et al. Dynamics of fat cell turnover in humans. Nature. 2008; 453:783–7. https://doi.org/10.1038/nature06902 PMID: 18454136

2. Prins JB, O'Rahilly S. Regulation of adipose cell number in man. Clin Sci. 1997; 92:3–11. PMID: 9038586

3. Wang QA, Tao C, Gupta RK, Scherer PE. Tracking adipogenesis during white adipose tissue development, expansion and regeneration. Nat Med. 2013; 19:1338–44. PubMed Central PMCID: PMC4075943. https://doi.org/10.1038/nm.3324 PMID: 23995282

4. Tchoukalova YD, Votruba SB, Tchkonia T, Giorgadze N, Kirkland JL, Jensen MD. Regional differences in cellular mechanisms of adipose tissue gain with overfeeding. Proc Natl Acad Sci U S A. 2010; 107:18226–31. PubMed Central PMCID: PMC2964201. https://doi.org/10.1073/pnas.1005259107 PMID: 20921416

5. Rutkowski JM, Stern JH, Scherer PE. The cell biology of fat expansion. J Cell Biol. 2015; 208:501–12. PubMed Central PMCID: PMC4347644. https://doi.org/10.1083/jcb.201409063 PMID: 25733711

6. Lehr S, Hartwig S, Sell H. Adipokines: a treasure trove for the discovery of biomarkers for metabolic disorders. Proteomics Clin Appl. 2012; 6:91–101. https://doi.org/10.1002/prca.201100052 PMID: 22213627

7. Kusminski CM, Bickel PE, Scherer PE. Targeting adipose tissue in the treatment of obesity-associated diabetes. Nat Rev Drug Discov. 2016; 15:639–60. https://doi.org/10.1038/nrd.2016.75 PMID: 27256476

8. Bays HE. "Sick fat," metabolic disease, and atherosclerosis. Am J Med. 2009; 122:S26–37. https://doi.org/10.1016/j.amjmed.2008.10.015 PMID: 19110085

9. Poledne R, Kralova Lesna I, Cejkova S. Adipose tissue and atherosclerosis. Physiol Res. 2015; 64 Suppl 3:S395–402.

10. Lazar I, Clement E, Dauvillier S, Milhas D, Ducoux-Petit M, LeGonidec S, et al. Adipocyte Exosomes Promote Melanoma Aggressiveness through Fatty Acid Oxidation: A Novel Mechanism Linking Obesity and Cancer. Cancer Res. 2016; 76:4051–7. https://doi.org/10.1158/0008-5472.CAN-16-0651 PMID: 27216185

11. Hefetz-Sela S, Scherer PE. Adipocytes: impact on tumor growth and potential sites for therapeutic intervention. Pharmacol Ther. 2013; 138:197–210. PubMed Central PMCID: PMC3602387. https://doi.org/10.1016/j.pharmthera.2013.01.008 PMID: 23353703

12. Cooke D, Bloom S. The obesity pipeline: current strategies in the development of anti-obesity drugs. Nat Rev Drug Discov. 2006; 5:919–31. https://doi.org/10.1038/nrd2136 PMID: 17080028

13. Jang BC. Artesunate inhibits adipogeneis in 3T3-L1 preadipocytes by reducing the expression and/or phosphorylation levels of C/EBP-alpha, PPAR-gamma, FAS, perilipin A, and STAT-3. Biochem Biophys Res Commun. 2016; 474:220–5. https://doi.org/10.1016/j.bbrc.2016.04.109 PMID: 27109481

14. Jang MK, Jung MH. ATF3 represses PPARgamma expression and inhibits adipocyte differentiation. Biochem Biophys Res Commun. 2014; 454:58–64. https://doi.org/10.1016/j.bbrc.2014.10.028 PMID: 25445599

15. Song Y, Park HJ, Kang SN, Jang SH, Lee SJ, Ko YG, et al. Blueberry peel extracts inhibit adipogenesis in 3T3-L1 cells and reduce high-fat diet-induced obesity. PLoS One. 2013; 8:e69925. PubMed Central PMCID: PMC3723699. https://doi.org/10.1371/journal.pone.0069925 PMID: 23936120

16. Wong CP, Kaneda T, Morita H. Plant natural products as an anti-lipid droplets accumulation agent. J Nat Med. 2014; 68:253–66. PubMed Central PMCID: PMC3948524. https://doi.org/10.1007/s11418-014-0822-3 PMID: 24550097

17. Kim SH, Park HS, Lee MS, Cho YJ, Kim YS, Hwang JT, et al. Vitisin A inhibits adipocyte differentiation through cell cycle arrest in 3T3-L1 cells. Biochem Biophys Res Commun. 2008; 372:108–13. https://doi.org/10.1016/j.bbrc.2008.04.188 PMID: 18482581

18. Urs S, Turner B, Tang Y, Rostama B, Small D, Liaw L. Effect of soluble Jagged1-mediated inhibition of Notch signaling on proliferation and differentiation of an adipocyte progenitor cell model. Adipocyte. 2012; 1:46–57. PubMed Central PMCID: PMCPMC3661121. https://doi.org/10.4161/adip.19186 PMID: 23700510

19. Choi JW, Lee CW, Lee J, Choi DJ, Sohng JK, Park YI. 7,8-Dihydroxyflavone inhibits adipocyte differentiation via antioxidant activity and induces apoptosis in 3T3-L1 preadipocyte cells. Life Sci. 2016; 144:103–12. https://doi.org/10.1016/j.lfs.2015.11.028 PMID: 26631505

20. Park YK, Lee J, Hong VS, Choi JS, Lee TY, Jang BC. Identification of KMU-3, a novel derivative of gallic acid, as an inhibitor of adipogenesis. PLoS One. 2014; 9:e109344. PubMed Central PMCID: PMC4186852. https://doi.org/10.1371/journal.pone.0109344 PMID: 25285517

21. Desarzens S, Liao WH, Mammi C, Caprio M, Faresse N. Hsp90 blockers inhibit adipocyte differentiation and fat mass accumulation. PLoS One. 2014; 9:e94127. PubMed Central PMCID: PMC3976389. https://doi.org/10.1371/journal.pone.0094127 PMID: 24705830

22. He Y, Li Y, Zhang S, Perry B, Zhao T, Wang Y, et al. Radicicol, a heat shock protein 90 inhibitor, inhibits differentiation and adipogenesis in 3T3-L1 preadipocytes. Biochem Biophys Res Commun. 2013; 436:169–74. https://doi.org/10.1016/j.bbrc.2013.05.068 PMID: 23727383

23. Zhang Y, Huang C. Targeting adipocyte apoptosis: a novel strategy for obesity therapy. Biochem Biophys Res Commun. 2012; 417:1–4. https://doi.org/10.1016/j.bbrc.2011.11.158 PMID: 22172945

24. Herold C, Rennekampff HO, Engeli S. Apoptotic pathways in adipose tissue. Apoptosis. 2013; 18:911–6. https://doi.org/10.1007/s10495-013-0848-0 PMID: 23584726

25. Fischer-Posovszky P, Kukulus V, Zulet MA, Debatin KM, Wabitsch M. Conjugated linoleic acids promote human fat cell apoptosis. Horm Metab Res. 2007; 39:186–91. https://doi.org/10.1055/s-2007-970416 PMID: 17373632

26. Singh J, Kakkar P. Oroxylin A, a constituent of Oroxylum indicum inhibits adipogenesis and induces apoptosis in 3T3-L1 cells. Phytomedicine. 2014; 21:1733–41. https://doi.org/10.1016/j.phymed.2014.08.014 PMID: 25442284

27. Hirota K, Morikawa K, Hanada H, Nonaka M, Nakajima Y, Kobayashi M, et al. Effect of genistein and daidzein on the proliferation and differentiation of human preadipocyte cell line. J Agric Food Chem. 2010; 58:5821–7. https://doi.org/10.1021/jf903911e PMID: 20397699

28.   Park HJ, Yang JY, Ambati S, Della-Fera MA, Hausman DB, Rayalam S, et al. Combined effects of genistein, quercetin, and resveratrol in human and 3T3-L1 adipocytes. J Med Food. 2008; 11:773–83. https://doi.org/10.1089/jmf.2008.0077 PMID: 19053873

29.   Jun DY, Han CR, Lee JY, Park W, Choi MS, Woo MH, et al. Anti-adipogenic activity of 2-carbomethoxy-2,3-epoxy-3-prenyl-1,4-naphthoquinone from Rubia cordifolia L. J Med Food. 2011; 14:454–61. https://doi.org/10.1089/jmf.2010.1385 PMID: 21434777

30.   Dave S, Kaur NJ, Nanduri R, Dkhar HK, Kumar A, Gupta P. Inhibition of adipogenesis and induction of apoptosis and lipolysis by stem bromelain in 3T3-L1 adipocytes. PLoS One. 2012; 7:e30831. PubMed Central PMCID: PMC3265525. https://doi.org/10.1371/journal.pone.0030831 PMID: 22292054

31.   Yang JY, Della-Fera MA, Baile CA. Guggulsterone inhibits adipocyte differentiation and induces apoptosis in 3T3-L1 cells. Obesity. 2008; 16:16–22. https://doi.org/10.1038/oby.2007.24 PMID: 18223606

32.   Kim HK, Della-Fera MA, Hausman DB, Baile CA. Effect of clenbuterol on apoptosis, adipogenesis, and lipolysis in adipocytes. J Physiol Biochem. 2010; 66:197–203. https://doi.org/10.1007/s13105-010-0024-8 PMID: 20535649

33.   Mendes V, Monteiro R, Pestana D, Teixeira D, Calhau C, Azevedo I. Xanthohumol influences preadipocyte differentiation: implication of antiproliferative and apoptotic effects. J Agric Food Chem. 2008; 56:11631–7. https://doi.org/10.1021/jf802233q PMID: 19035642

34.   Rayalam S, Yang JY, Ambati S, Della-Fera MA, Baile CA. Resveratrol induces apoptosis and inhibits adipogenesis in 3T3-L1 adipocytes. Phytother Res. 2008; 22:1367–71. https://doi.org/10.1002/ptr.2503 PMID: 18688788

35.   Humphrey S, Sykes J, Kantor J, Bertucci V, Walker P, Lee DR, et al. ATX-101 for reduction of submental fat: A phase III randomized controlled trial. J Am Acad Dermatol. 2016; 75:788–97.e7. https://doi.org/10.1016/j.jaad.2016.04.028 PMID: 27430612

36.   Wollina U, Goldman A. ATX-101 for reduction of submental fat. Expert Opin Pharmacother. 2015; 16:755–62. https://doi.org/10.1517/14656566.2015.1019465 PMID: 25724831

37.   Dayan SH, Humphrey S, Jones DH, Lizzul PF, Gross TM, Stauffer K, et al. Overview of ATX-101 (Deoxycholic Acid Injection): A Nonsurgical Approach for Reduction of Submental Fat. Dermatol Surg. 2016; 42 Suppl 1:S263–S70.

38.   Rotunda AM. Injectable treatments for adipose tissue: terminology, mechanism, and tissue interaction. Lasers Surg Med. 2009; 41:714–20. https://doi.org/10.1002/lsm.20807 PMID: 20014257

39.   Mizutani T. Toxicity of xanthene food dyes by inhibition of human drug-metabolizing enzymes in a non-competitive manner. J Environ Public Health. 2009; 2009:953952. PubMed Central PMCID: PMCPMC2778353. https://doi.org/10.1155/2009/953952 PMID: 20041016

40.   Rewcastle GW, Atwell GJ, Palmer BD, Boyd PD, Baguley BC, Denny WA. Potential antitumor agents. 62. Structure-activity relationships for tricyclic compounds related to the colon tumor active drug 9-oxo-9H-xanthene-4-acetic acid. J Med Chem. 1991; 34:491–6. PMID: 1995870

41.   Combes RD, Haveland-Smith RB. A review of the genotoxicity of food, drug and cosmetic colours and other azo, triphenylmethane and xanthene dyes. Mutat Res. 1982; 98:101–248. PMID: 7043261

42.   Kim JR, Michielsen S. Synthesis of Antifungal Agents from Xanthene and Thiazine Dyes and Analysis of Their Effects. Nanomaterials (Basel). 2016; 6. PubMed Central PMCID: PMCPMC5302722.

43.   Agarwala S, Wachter E. Rose bengal: from a wool dye to a cancer therapy. P T. 2010; 35:474–78. PubMed Central PMCID: PMCPMC2935646.

44.   Kim YS, Rubio V, Qi J, Xia R, Shi ZZ, Peterson L, et al. Cancer treatment using an optically inert Rose Bengal derivative combined with pulsed focused ultrasound. J Control Release. 2011; 156:315–22. PubMed Central PMCID: PMCPMC3230682. https://doi.org/10.1016/j.jconrel.2011.08.016 PMID: 21871506

45.   Lim YW, Sanz LA, Xu X, Hartono SR, Chedin F. Genome-wide DNA hypomethylation and RNA:DNA hybrid accumulation in Aicardi-Goutieres syndrome. Elife. 2015; 4. PubMed Central PMCID: PMCPMC4528086.

46.   Livak KJ, Schmittgen TD. Analysis of relative gene expression data using real-time quantitative PCR and the 2(-Delta Delta C(T)) Method. Methods. 2001; 25:402–8. https://doi.org/10.1006/meth.2001.1262 PMID: 11846609

47.   Li H, Lee JH, Kim SY, Yun HY, Baek KJ, Kwon NS, et al. Phosphatidylcholine induces apoptosis of 3T3-L1 adipocytes. J Biomed Sci. 2011; 18:91. PubMed Central PMCID: PMC3261832. https://doi.org/10.1186/1423-0127-18-91 PMID: 22145579

48.   Cristancho AG, Lazar MA. Forming functional fat: a growing understanding of adipocyte differentiation. Nat Rev Mol Cell Biol. 2011; 12:722–34. https://doi.org/10.1038/nrm3198 PMID: 21952300